

CdSe/ZnS Core/Shell Quantum Dot Sensitization of Low Index TiO₂ Single Crystal Surfaces

Justin B. Sambur^{†,‡} and B. A. Parkinson^{*,‡}

Department of Chemistry, Colorado State University, Fort Collins, Colorado 80523, and Department of Chemistry and School of Energy Resources, University of Wyoming, Laramie, Wyoming 82071

Received November 30, 2009; E-mail: bparkin1@uwyo.edu

Quantum dots (QDs) or semiconductor nanocrystals are actively being explored as sensitizers in sensitized solar cells. QDs may offer the advantages of enhanced stability compared to conventional dyes, as well as high light absorption that can be tuned to cover a large fraction of the solar spectrum simply by changing their size.^{1,2} Despite such beneficial attributes quantum dot sensitized solar cells (QDSSCs) have not achieved efficiencies or stabilities competitive with conventional dye sensitized solar cells. This is at least partially due to a lack of fundamental understanding of the surface chemistry of QD adsorption in nanocrystalline TiO₂ films that leads to low QD coverages (<50%) on the nanoporous materials.³ Furthermore the structure and distribution of QDs on nanocrystalline TiO₂ surfaces is difficult to determine since the surface is not flat and mostly inaccessible to scanning probes and electron beams. Herein we address structure and stability issues associated with QD sensitization by using single crystal semiconducting oxide surfaces as model interfaces to study the sensitization yields and surface structures for both 3-mercaptopropionic acid (MPA) capped core CdSe QDs (core-QDs) and MPA capped CdSe/ZnS core shell (CS-QDs).

The atomically flat rutile (001) TiO₂ surface shown in the tapping mode atomic force microscopy (AFM) image (Figure 1a) allows us to evaluate if the QD coverage is uniform or dominated by 2D or 3D clusters as we and others have previously observed.⁴ We recently determined that reproducible monolayer coverages of CdSe QDs covalently bound to single crystal TiO₂ surfaces was governed by both QD purity and the pH of treatment solutions.⁴ QDs purified to remove surfactants and dispersed in basic (pH 10.2) aqueous solutions enable MPA ligands to form stable thiolate-Cd chemical bonds (pK_a^{SH} of MPA = 10.2) without excess MPA in solution and reproducibly result in QD-TiO₂ attachment (see Supporting Information for experimental details).⁵ The AFM image in Figure 1b shows a rutile (001) surface covered with core-QDs. Figure 1c and 1d show a large area and high-resolution scan of a rutile (110) surface after CS-QD adsorption, respectively. The height profiles measured in Figure 1b and 1c indicate respective 3.5 and 5.0 nm z-heights of the QDs above the bare TiO₂ surface. Due to tip effects it is difficult to accurately determine the particle diameter directly from *x*-*y* measurements, but it is clear from the high resolution AFM image in Figure 1d that large structures arise from clusters of individual QDs rather than large nanocrystals.

The optical absorption spectra of core CdSe and CS-QDs in water are shown in Figure 2a. The 1S_{3/2}-1S_e absorption maxima at 577 nm for the core-QDs corresponds to a diameter of ~3.8 nm, in good agreement with primarily a core-QD monolayer determined via AFM.⁶ To determine the CS-QD particle diameter, the monolayer thickness of the ZnS shell was calculated according to the

3.1 Å distance between consecutive planes along the [002] axis in bulk wurtzite ZnS.⁷ According to the manufacturer, a 2 to 3 ML ZnS shell was epitaxially grown in solution on a 4.0 nm CdSe core. Therefore the average CS-QD diameter ranges from 5.2 to 5.9 nm, which is also in good agreement with the AFM results for CS-QDs. Therefore the sensitization conditions primarily result in a single layer of core and CS-QDs with some agglomerated structures consisting of two particles stacked in the *z* direction.

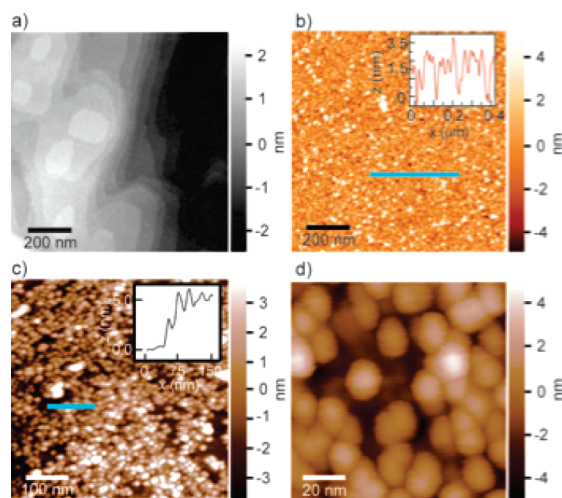


Figure 1. AFM images of (a) bare rutile (001), (b) core CdSe QDs on rutile (110), (c) and (d) CS-QDs adsorbed on the same rutile (001) surface. The teal bars indicate regions representing the height profiles.

The incident photon to current efficiency (IPCE) spectra (Figure 2a) of core CdSe and CS-QDs on an anatase (001) electrode surface in an aqueous iodide electrolyte mimics the corresponding solution absorbance spectra and exhibited similar IPCE values. Sensitization of TiO₂ with CS-QDs is distinguished by an additional peak at 550 nm as well as a distinct red shift and broadening in the first exciton peak due to partial overlap of the exciton wave function with the ZnS shell.⁷ To the best of our knowledge, this is the first demonstration of sensitizing TiO₂ with colloidal solutions of core/shell QDs. Similar results were obtained on other low index anatase and rutile crystals (Figure S1).

The energy level diagram in the inset of Figure 2b shows type-I band alignment whereby the conduction and valence band (CB and VB) positions of ZnS result in a potential energy barrier for electrons to inject into the CB of TiO₂ and for holes to inject into the electrolyte. Type-I CS-QDs energy alignments produce a quantum well usually favoring exciton recombination and luminescence rather than dissociation.⁸ Thus the potential barriers for charge carrier separation from the band alignment in Figure 2b suggests that type-I CS-QDs would not be effective at injecting

[†] Colorado State University.

[‡] University of Wyoming.

electrons into TiO_2 . However, recent experiments by Lian and co-workers reported an average electron transfer rate from single 4.0 nm CdSe/ZnS QDs coated with an ~ 4 nm amphiphilic polymer to TiO_2 nanoparticles of $3.2 \times 10^7 \text{ s}^{-1}$, slower than the $6.3 \times 10^8 \text{ s}^{-1}$ electron transfer rate reported for 3.7 nm CdSe core QDs.^{9,10} Likewise, Makhal et al. recently reported electron transfer rates of $3.3 \times 10^9 \text{ s}^{-1}$ and $2.9 \times 10^8 \text{ s}^{-1}$ for 2.4 and 4.2 nm diameter CdSe/ZnS CS-QDs respectively, which are comparable to core CdSe QDs.¹¹ Additionally, hole injection into a sulfide electrolyte was not inhibited from ZnS-coated CdSe QDs deposited on TiO_2 inverse opals (chemical bath deposited ZnS only on the outer exposed surface of CdSe QDs).¹² Despite the type-I CS structure, experimental results suggest the overlap between electron and hole wave functions of CdSe/ZnS QDs and the TiO_2 CB and regenerator orbitals is sufficient for charge separation.

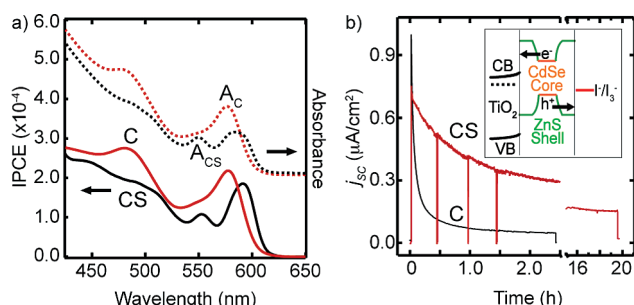


Figure 2. (a) Solid lines represent IPCE spectra of core (C) and core/shell (CS) MPA-capped CdSe QDs adsorbed on an anatase (001) electrode surface measured in an aqueous iodide (0.25 M KI) electrolyte at short circuit versus a Pt wire. The corresponding solution absorbance spectrum (dashed lines) of the core (A_C) and CS (A_{CS}) QD samples in water are also shown. (b) Photocurrent versus time of C and CS QDs adsorbed on an anatase (001) electrode surface with $47.7 \text{ mW}/\text{cm}^2$ illumination at 532 nm. The spikes on trace CS result from momentary blocking of the light. The inset shows an illustration of the pathway for electrons and holes for photoexcited CS-QDs.

Although the interfacial electronic structure of TiO_2 /type-I CS-QDs/electrolyte seems unfavorable for sensitized solar cells, the stable, wide band gap shell material should result in improved device stability. Cadmium chalcogenide photoanodes are generally unstable in aqueous and organic iodide-based electrolytes due to rapid metal iodide formation leading to degradation.¹ Figure 2b shows a short circuit photocurrent stability test ($47.7 \text{ mW}/\text{cm}^2$ of 532 nm laser light or ~ 0.5 sun) of core and CS-QDs adsorbed on an anatase (001) surface in an aerated iodide electrolyte. The photocurrent of the core-QDs decayed by half ($\tau_{1/2}$) in 2.4 min and after 2.4 h had decayed by over 90%, whereas for CS-QDs $\tau_{1/2}$ was 84.1 min but 21.2% of the initial photocurrent signal was retained even after 20 h of continuous illumination. Both the core and CS-QDs are stable for extended periods (>30 h) in sulfide/polysulfide electrolytes routinely used to stabilize cadmium chalcogenide photoanodes. The normalized IPCE spectra of the CS-QDs taken before and after the stability test were similar, whereas the IPCE spectrum of the cores was entirely different (Figures S2 and S3). The distinct blue shift in the IPCE spectrum of the core QD/ TiO_2 system suggests an increase in the band gap of the QDs.

This can be explained by a 1.8 nm decrease in particle diameter according to the energy position of the first exciton peak as a result of decomposition of the CdSe core by reaction with I^- or I_3^- to form CdI_2 .⁶

An alternative explanation for the sensitization currents measured for the CS-QDs is that electron injection occurs only when defects in the ZnS shell from the synthesis or ligand exchange allow the CdSe core to directly contact the TiO_2 surface. Despite a decrease in the quantum yield upon transfer to the aqueous phase, the solution absorbance and luminescence spectra of the CS-QDs before and after ligand exchange did not exhibit significant spectral shifts, suggesting the ZnS shell remained intact (Figure S4). The AFM images indicated monolayer coverage for both core and CS-QDs, and the comparable IPCE spectra (Figure 1a) on the same anatase (001) surface suggest that the majority of intact CS-QDs are injecting. In addition the CS-QDs are stable and retain the same IPCE spectral features (Figure S3) in an aqueous iodide electrolyte long after the photocurrent from the core QDs has completely decayed. These observations clearly demonstrate that intact type-I CS CdSe/ZnS QDs produced the sensitized photocurrents.

The results presented herein may have important implications for a variety of QD or nanoparticle materials previously found to be unstable in sensitized solar cells. For instance type-II CS QD materials may improve charge separation and limit recombination by promoting the forward electron transfer reactions while limiting the reverse processes due to the spatial separation of the electron and hole in different regions of the type-II CS-QD.⁸ The possibility of exploring new core/shell nanomaterials in a variety of electrolyte/mediator combinations may result in more efficient and stable QDSSCs.

Acknowledgment. We thank Jason Li and Mario Viani of Asylum Research for assistance with AFM images. This work was funded by the DOE-BES Grant No. DE-FG03-96ER14625.

Supporting Information Available: Experimental methods, IPCE spectra of CS-QDs on anatase (101) and rutile (110), normalized IPCE spectra of core and CS-QDs after stability test, and CS-QD absorption spectra before and after ligand exchange. This material is available free of charge via the Internet at <http://pubs.acs.org>.

References

- (1) Hodes, G. J. *Phys. Chem. C* **2008**, *112*, 17778.
- (2) Kamat, P. V. *J. Phys. Chem. C* **2008**, *112*, 18737.
- (3) Mora-Seró, I.; Giménez, S.; Fabregat-Santiago, F.; Gómez, R.; Shen, Q.; Toyoda, T.; Bisquert, J. *Acc. Chem. Res.* **2009**, *42*, 1848.
- (4) Sambur, J. B.; Riha, S. C.; Choi, D.; Parkinson, B. A. *Langmuir*, accepted.
- (5) Aldana, J.; Lavelle, N.; Wang, Y. A.; Peng, X. G. *J. Am. Chem. Soc.* **2005**, *127*, 2496.
- (6) Yu, W. W.; Qu, L. H.; Guo, W. Z.; Peng, X. G. *Chem. Mater.* **2003**, *15*, 2854.
- (7) Dabbousi, B. O.; Rodriguez-Viejo, J.; Mikulec, F. V.; Heine, J. R.; Mattoussi, H.; Ober, R.; Jensen, K. F.; Bawendi, M. G. *J. Phys. Chem. B* **1997**, *101*, 9463.
- (8) Reiss, P.; Protiere, M.; Li, L. *Small* **2009**, *5*.
- (9) Jin, S.; Lian, T. *Nano Lett.* **2009**, *9*, 2448.
- (10) Kongkanand, A.; Tvrdy, K.; Takechi, K.; Kuno, M.; Kamat, P. *J. Am. Chem. Soc.* **2008**, *130*, 4007.
- (11) Makhal, A.; Yan, H.; Lemmens, P.; Pal, S. K. *J. Phys. Chem. C* **2009**, *114*, 627.
- (12) Shen, Q.; Kobayashi, J.; Diguna, L. J.; Toyoda, T. *J. Appl. Phys.* **2008**, *103*, 084304/1.

JA9098577